Supporting Information

ATP Can Efficiently Stabilize Protein through a Unique Mechanism

Xinwen Ou,[a,⊥] Yichong Lao,[a,⊥] Jingjie Xu,[b,⊥] Yanee Wutthinitikornkit,[a] Rui Shi,[a] Xiangjun Chen,[b,*] Jingyuan Li[a,*]

[a]Zhejiang Province Key Laboratory of Quantum Technology and Device, Department of Physics, Zhejiang University, Zheda Road 38, Hangzhou 310027, China.
[b]Eye Center of the Second Affiliated Hospital, Institute of Translational Medicine, School of Medicine, Zhejiang University, Hangzhou 310009, China.
[⊥]These authors contributed equally.
[*]Email: chenxiangjun@zju.edu.cn or jingyuanli@zju.edu.cn.

Table S1. The residue in ATP-susceptible and ATP-neutral region of lysozyme in a representative trajectory, and the positively-charged and negatively-charged residues are marked in red and blue respectively. The shaded area represents a relatively continuous ATP-susceptible region.

ATP-susceptible region	4G, 5R, 6C, 10A, 14R, 33K, 34F, 37N, 38F, 39N, 41Q, 42A, 43T, 44N, 45R, 46N, 47T, 48D, 49G, 50S, 51T, 52D, 59N, 60S, 61R, 62W, 63W, 66D, 68R, 69T, 98I, 101D, 102G, 107A, 108W, 109V, 114R, 125R, 126G, 127C, 128R, 129L
ATP-neutral region	1K, 2V, 3F, 7E, 8L, 9A, 11A, 12M, 13K, 15H, 16G, 17L, 18D, 19N, 20Y, 21R, 22G, 23Y, 24S, 25L, 26G, 27N, 28W, 29V, 30C, 31A, 32A, 35E, 36S, 40T, 53Y, 54G, 55I, 56L, 57Q, 58I, 64C, 65N, 67G, 70P, 71G, 72S, 73R, 74N, 75L, 76C, 77N, 78I, 79P, 80C, 81S, 82A, 83L, 84L, 85S, 86S, 87D, 88I, 89T, 90A, 91S, 92V, 93N, 94C, 95A, 96K, 97K, 99V, 100S, 103N, 104G, 105M, 106N, 110A, 111W, 112R, 113N, 115C, 116K, 117G, 118T, 119D, 120V, 121Q, 122A, 123W, 124I

Table S2. The residue in ATP-susceptible region of ubiquitin in a representative trajectory, and the positively-charged and negatively-charged residues are marked in red and blue respectively. The shaded area represents a relatively continuous ATP-susceptible region.

ATP-susceptible region	24E, 39D, 40Q, 42R, 47G, 48K, 49Q, 51E, 52D, 53G, 54R, 55T, 58D, 72R, 73L, 74R, 75G, 76G

Table S3. The residue in ATP-susceptible region of malate dehydrogenase in a representative trajectory, and the positively-charged and negatively-charged residues are marked in red and blue respectively. The shaded area represents a relatively continuous ATP-susceptible region.

ATP-susceptible region	1S, 2E, 3P, 31K, 32D, 33Q, 34P, 63L, 109K, 138T, 141K, 142S, 254R, 257W, 258F, 259G, 260T, 261P, 262E, 282D, 292K, 293D, 294K, 326A, 327F, 328E, 330L, 331S, 332S, 338R, 364K, 399D, 400V, 401I, 402A, 403T, 408I, 411K, 412D, 424R, 427G, 428M, 429E, 430R, 432D, 474K, 481K, 498Q, 501L, 502K, 503L, 545V, 546K, 550W, 558T, 561Q, 564A, 567I, 568K, 571K, 606D, 615D, 654E

Table S4. The details of the simulated systems, the initial distance between the protein and the box edge is larger than 3 nm for each system.

System	Initial box size	ATP-Mg	Water molecules	Sodium ions	Chloride ions
Lysozyme	12.6 × 12.6 × 12.6 nm^3	0	63083	181	189
Lysozyme in pure water	12.6 × 12.6 × 12.6 nm^3	0	63445	0	8
Lysozyme and $MgCl_2$	12.6 × 12.6 × 12.6 nm^3	0 ATP, 20 Mg^{2+}	63023	181	229
Lysozyme and ATP	12.6 × 12.6 × 12.6 nm^3	20 ATP, 0 Mg^{2+}	62653	253	181
Ubiquitin	10.0 × 10.0 × 10.0 nm^3	0	32216	90	90
Malate dehydrogenase	14.4 × 14.4 × 14.4 nm^3	0	95712	274	270
ATP-Mg	12.6 × 12.6 × 12.6 nm^3	20	63299	221	181
Lysozyme and ATP-Mg	12.6 × 12.6 × 12.6 nm^3	20	62677	213	181
Ubiquitin and ATP-Mg	10.0 × 10.0 × 10.0 nm^3	10	31981	110	90
Malate dehydrogenase and ATP-Mg	14.4 × 14.4 × 14.4 nm^3	30	95079	334	270

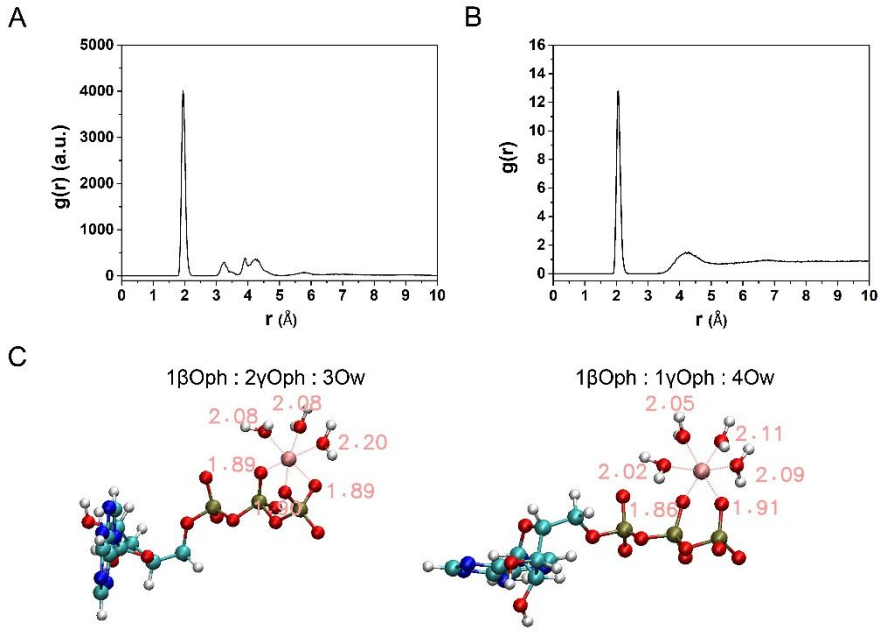

Figure S1. Radial distribution functions, g(r), of ATP phosphate oxygens (A) and water oxygens (B) around Mg^{2+} in ATP-Mg solution. (C) Representative snapshots depicting the coordination of ATP phosphate groups and water molecules with Mg^{2+}. The average coordination distances for Mg-Ow (water oxygens) and Mg-Oph (phosphate oxygens) are 2.04 Å and 1.94 Å respectively, and the average coordination numbers of Mg^{2+} with Ow and Oph are 3.45 and 2.51 respectively. Atoms are colored as follows: Mg (pink), C (cyan), O (red), N (blue), P (tan), and H (white). The analyses are based on the last 50-ns trajectory.

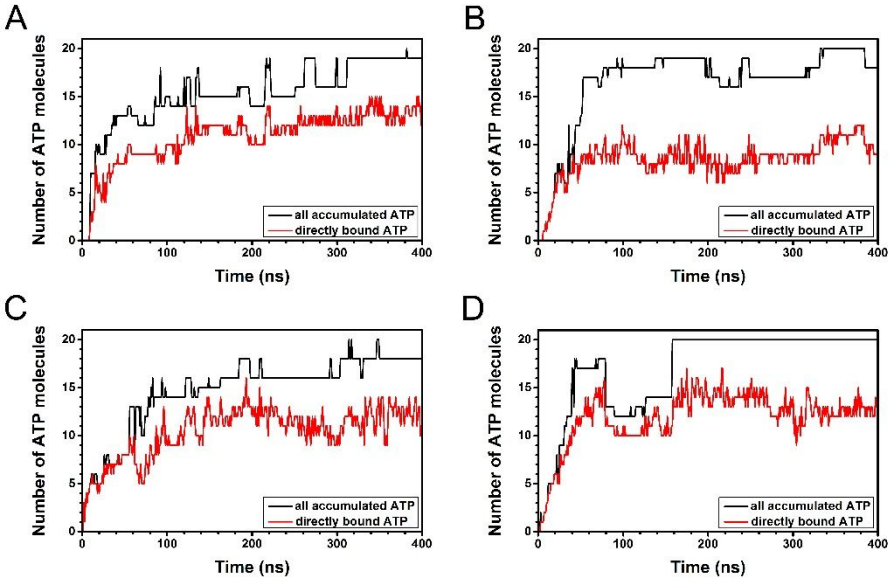

Figure S2. The number of ATPs accumulated around lysozyme for the other four trajectories.

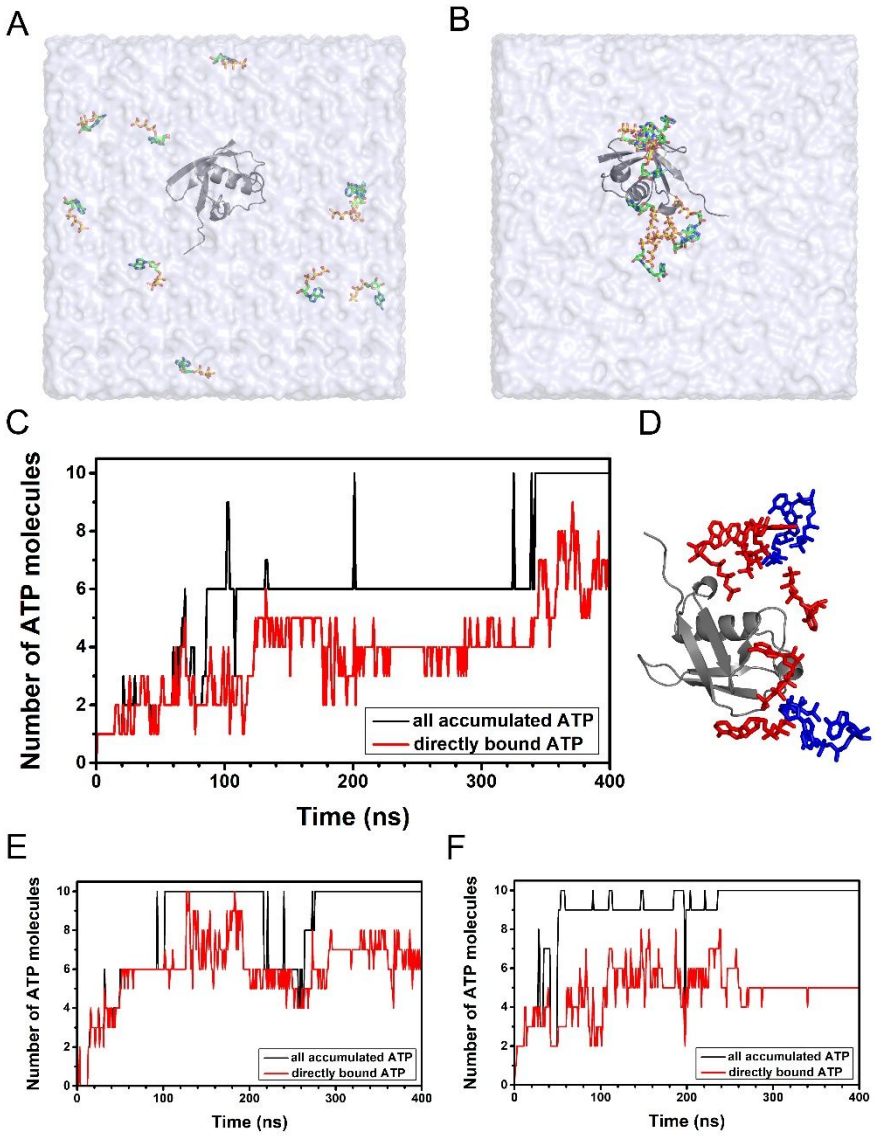

Figure S3. Binding and accumulation of ATP around ubiquitin. (A-B) Initial and final configurations of the ATP binding to protein. (C) The number of ATPs accumulated around protein (D) ATPs in direct (in red) and indirect (in blue) contact with protein. (E-F) The number of ATPs accumulated around protein for the other two trajectories.

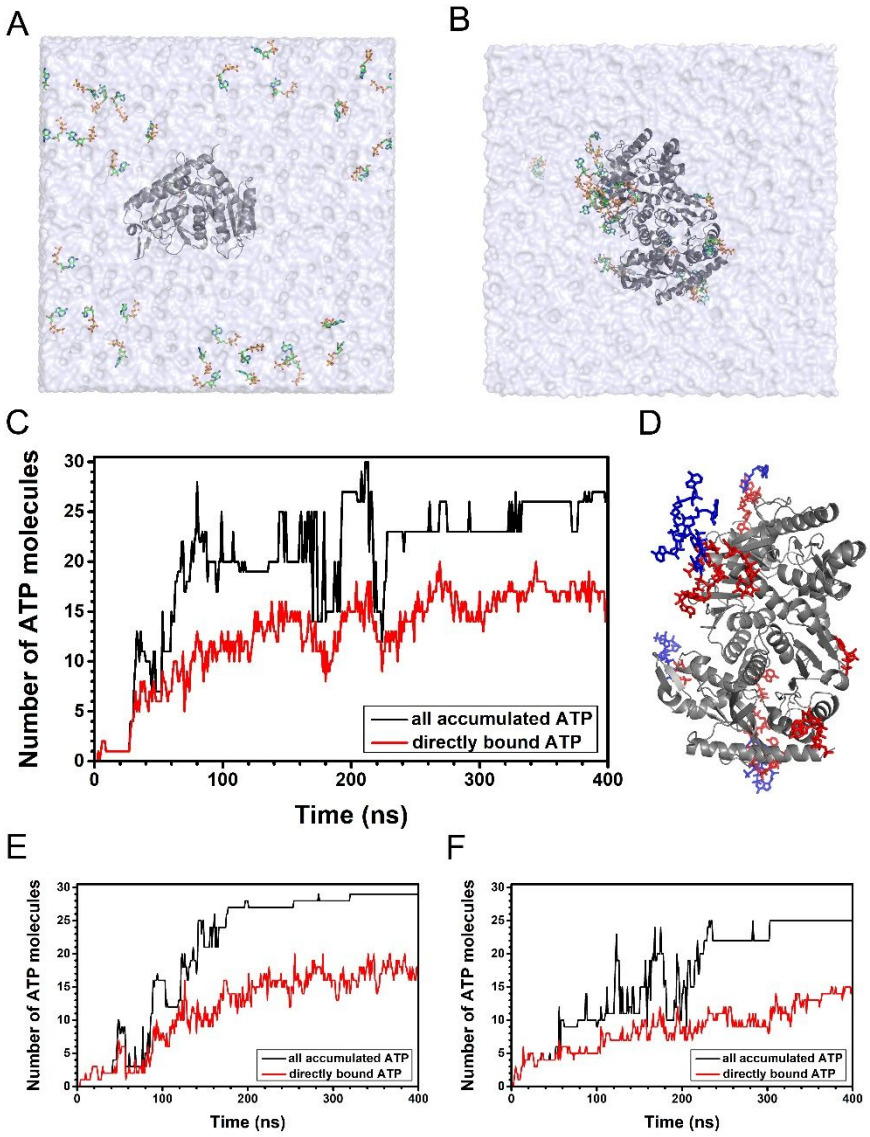

Figure S4. Binding and accumulation of ATP around malate dehydrogenase. (A-B) Initial and final configurations of the ATP binding to protein. (C) The number of ATPs accumulated around protein (D) ATPs in direct (in red) and indirect (in blue) contact with protein. (E-F) The number of ATPs accumulated around protein for the other two trajectories.

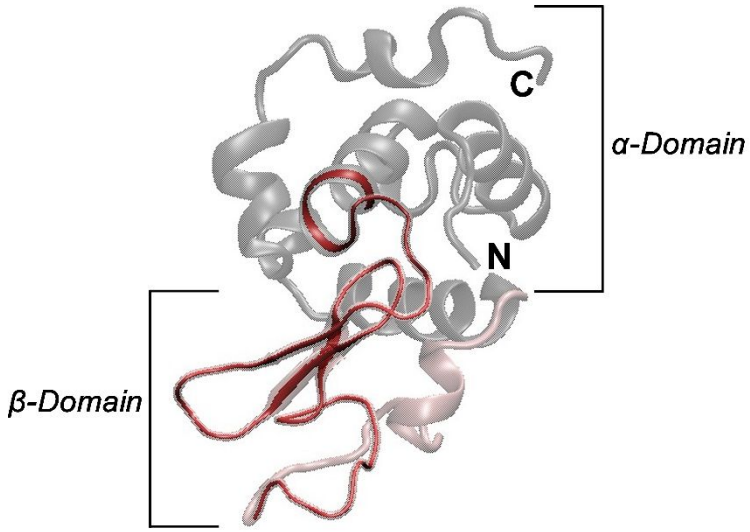

Figure S5. The schematic representation of the structure of lysozyme, which consists of α-domain (colored in grey, residues: 1-39 and 88-129) and β-domain (colored in pink, residues: 40-87). The inter-domain loop (residues: 33-70) is colored in red.

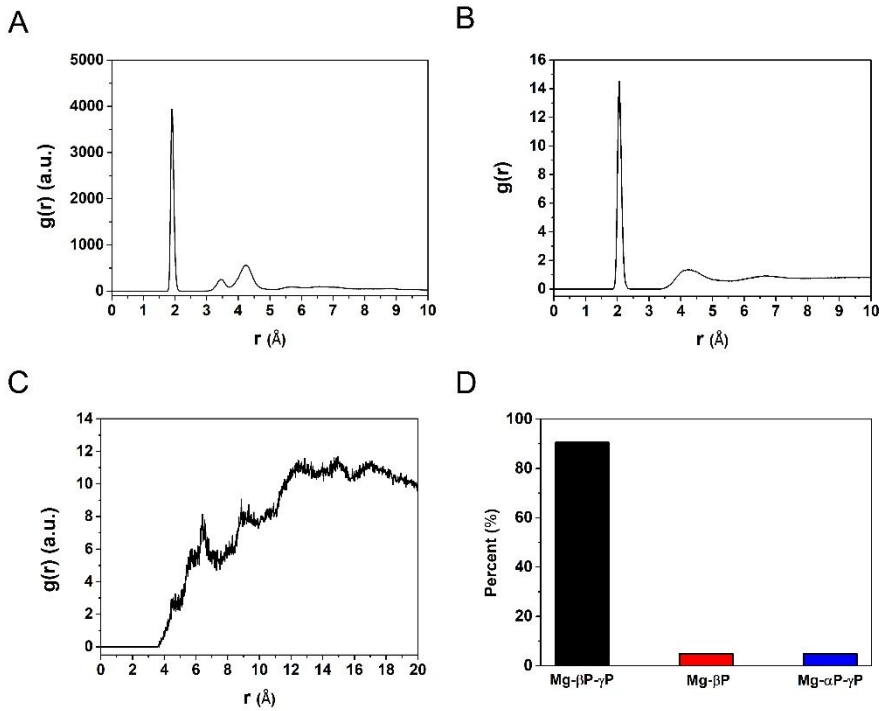

Figure S6. Radial distribution functions, g(r), of ATP phosphate oxygens (A), water oxygens (B), and N, O atoms of lysozyme (C) around Mg^{2+}. (D) Histogram showing the population of each coordination mode of ATP-Mg complex. The average coordination distances for Mg-Ow and Mg-Oph are 2.06 Å and 1.90 Å respectively, and the average coordination numbers of Mg^{2+} with Ow and Oph is 3.95 and 2.05 respectively. The analyses are based on the last 160-ns trajectory.

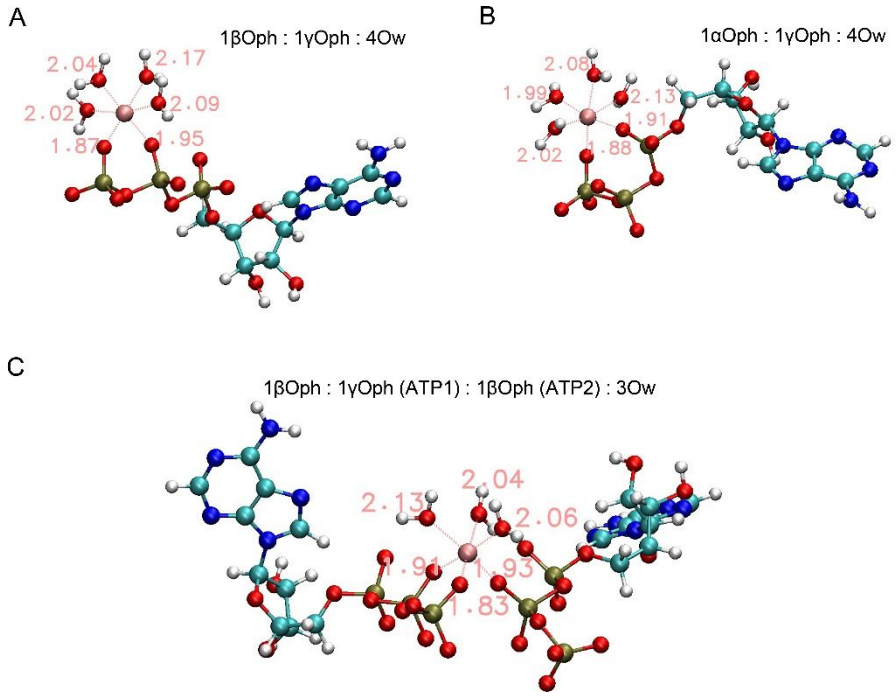

Figure S7. Representative snapshots depicting the coordination of ATP phosphate groups and water molecules with Mg^{2+} within the ATP-clusters on lysozyme.

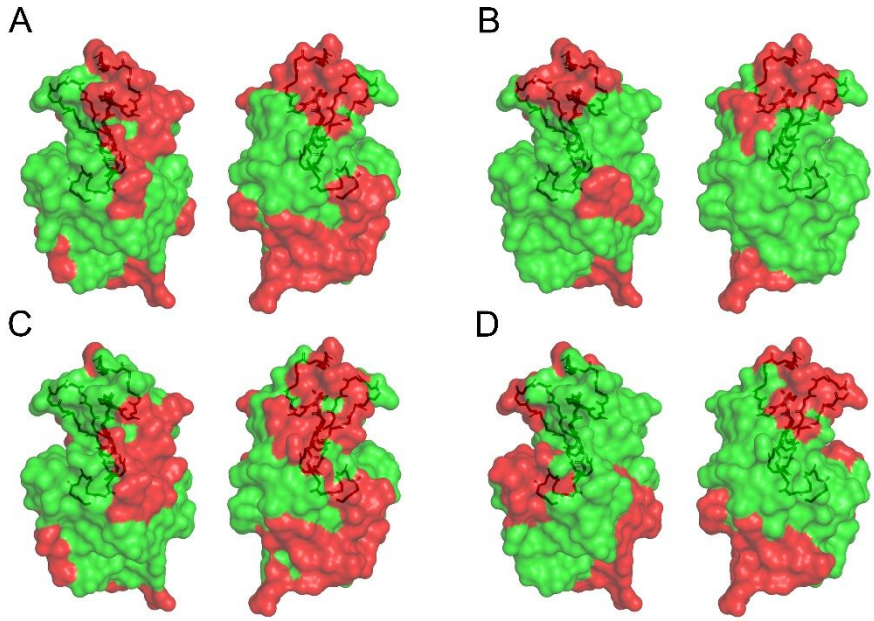

Figure S8. ATP-susceptible (red) and ATP-neutral (green) regions of lysozyme for the other four trajectories of ATP-Mg solution, the inter-domain loop is shown in sticks.

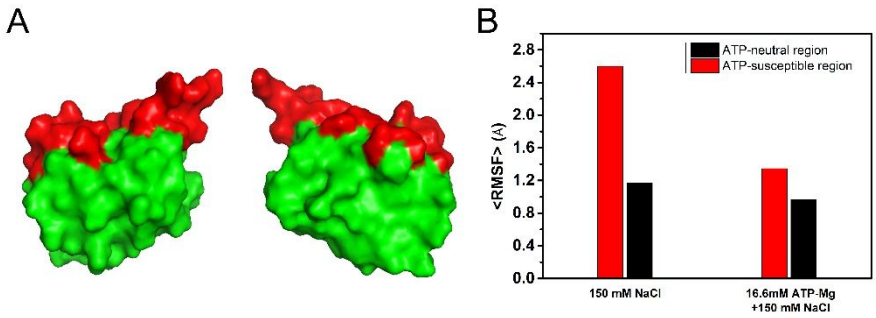

Figure S9. ATP binding reduces the structural fluctuations of ubiquitin. (A) ATP-susceptible (red) and ATP-neutral (green) regions of ubiquitin. (B) The average RMSF of the residues in the ATP-susceptible and ATP-neutral region.

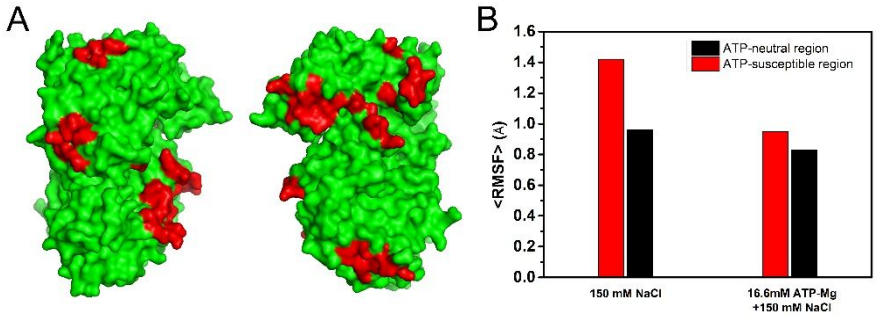

Figure S10. ATP binding reduces the structural fluctuations of malate dehydrogenase. (A) ATP-susceptible (red) and ATP-neutral (green) regions of malate dehydrogenase. (B) The average RMSF of the residues in the ATP-susceptible and ATP-neutral region.

Lysozyme: K33-T69

KFESNFNTQATNRNTDGSTDYGILQINSRWWCNDGRT

Sequence identity with Malate Dehydrogenase: 16.13% (calculated by CLUSTAL 2.1)

Ubiquitin: D39-D58

D Q Q R L I F A G K Q L E D G R T L S D

Sequence identity with Malate Dehydrogenase: 25.00% (calculated by CLUSTAL 2.1)

Malate Dehydrogenase: D399-D432

DVIATDKEEIAFKDLDVAILVGSMPRRDGMERKD

Sequence identity with Malate Dehydrogenase: --

Figure S11. The sequence identities of the amino acid segments corresponding to the vulnerable regions of lysozyme, ubiquitin, and malate dehydrogenase.

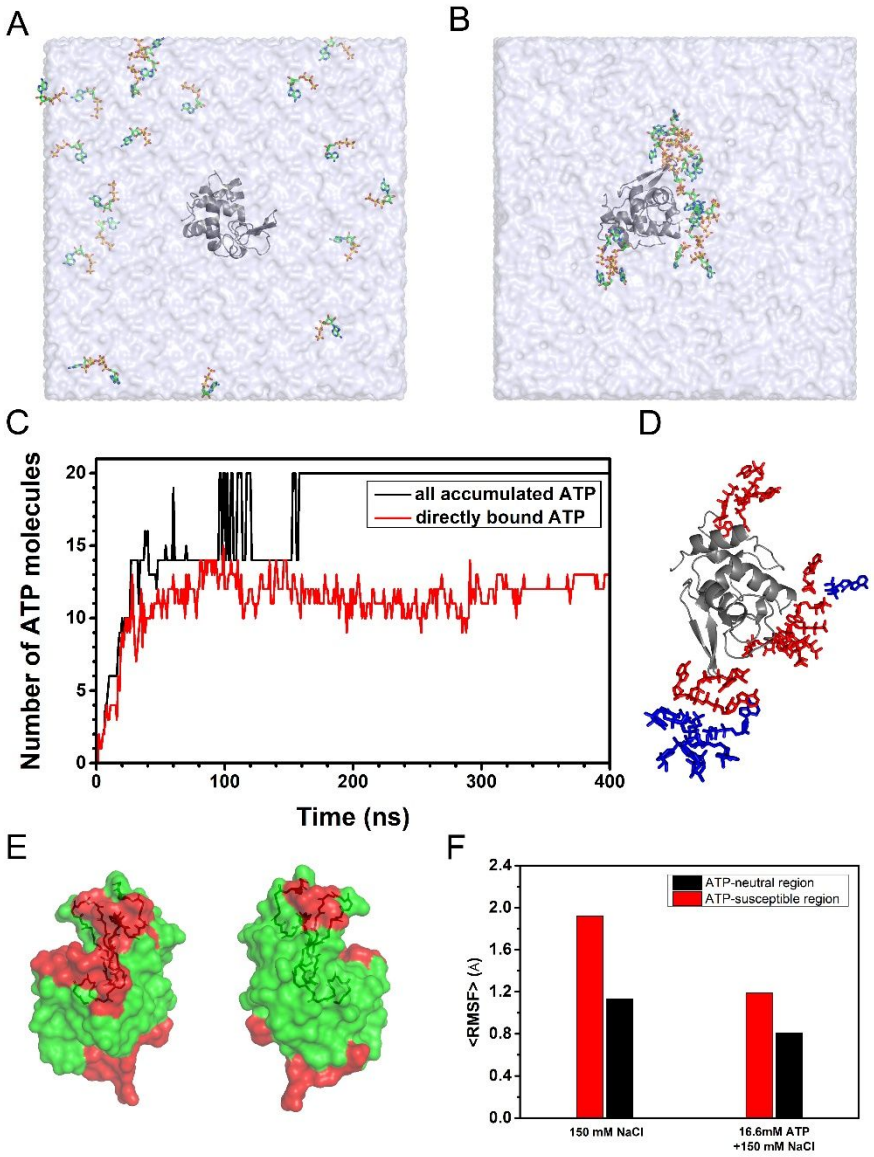

Figure S12. Binding and accumulation of ATP around lysozyme in Mg^{2+}-free ATP solution (150 mM NaCl). (A-B) Initial and final configurations of the ATP binding to protein. (C) The number of ATPs accumulated around protein (D) ATPs in direct (in red) and indirect (in blue) contact with protein. (E) ATP-susceptible (red) and ATP-neutral (green) regions of lysozyme, the inter-domain loop is shown in sticks. (F) The average RMSF of the residues in the ATP-susceptible and ATP-neutral region.

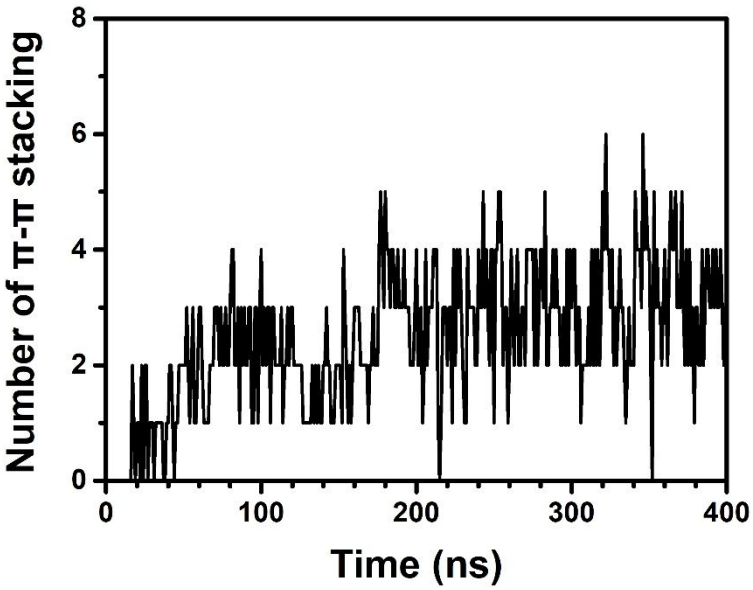

Figure S13. The number of π-π stacking interactions between the accumulated ATPs (the COM distance between two adenine bases is less than 5 Å) in *Mg^{2+}-free ATP solution*.

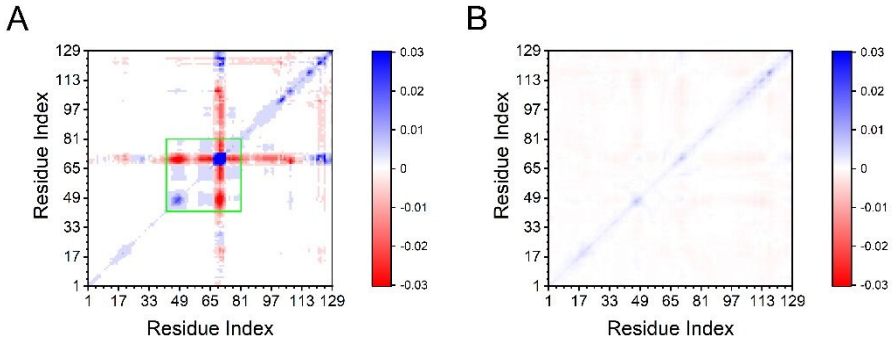

Figure S14. The dynamical cross-correlation matrices of the C-alpha atoms of free lysozyme (A, 150 mM NaCl) and ATP-bound lysozyme (B, 16.6 mM ATP-Mg, based on the last 160-ns trajectory). The positive covariance *Cij* suggests a correlated motion between the residue *i* and *j*, whereas the negative covariance suggests an anti-correlated motion. The areas in blue and red correspond to the correlated and anti-correlated motions, respectively. The region with strong cross-correlation motions is highlighted in the green box. The color scale is in nm^2.

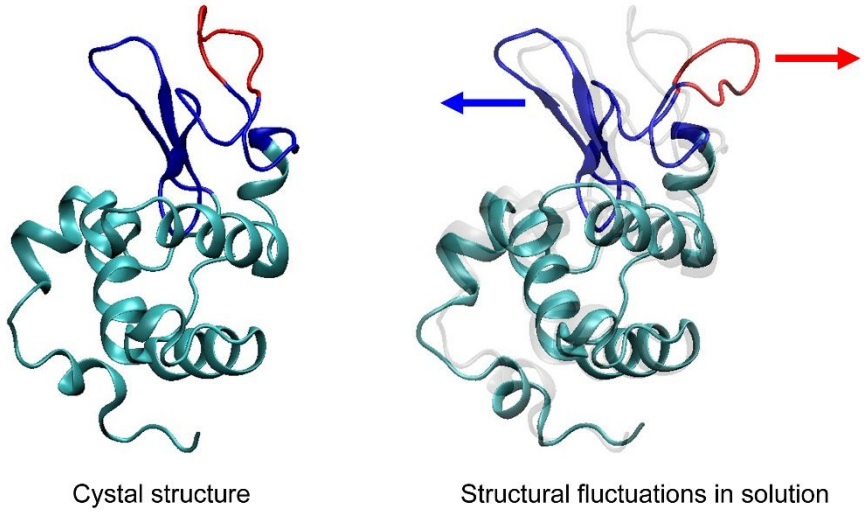

Figure S15. Snapshots illustrating the structural fluctuation of free lysozyme in 150 mM NaCl solution. Residues 42-65, 75-81 are shown in blue (correlated movements), 66-74 in red (anti-correlated movements), other residues in cyan.

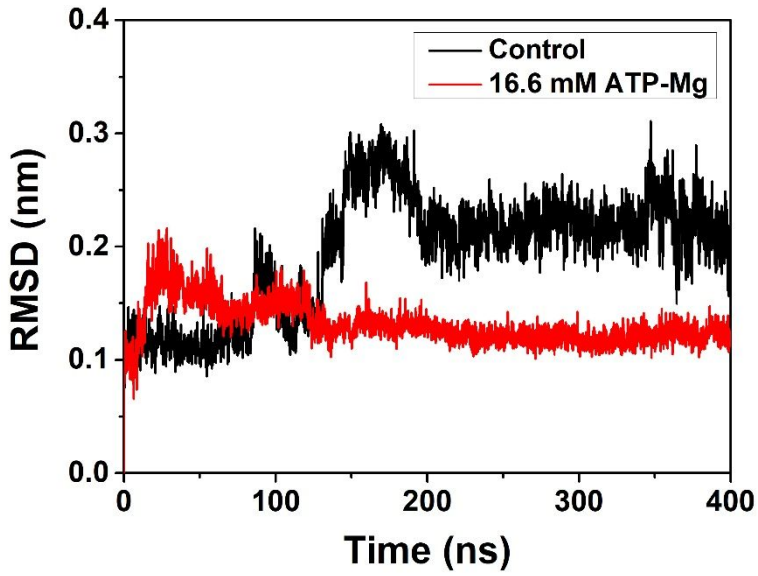

Figure S16. RMSD of backbone atoms with respect to the crystal structure for lysozyme in 150 mM NaCl solution and 16.6 mM ATP-Mg solution, respectively.

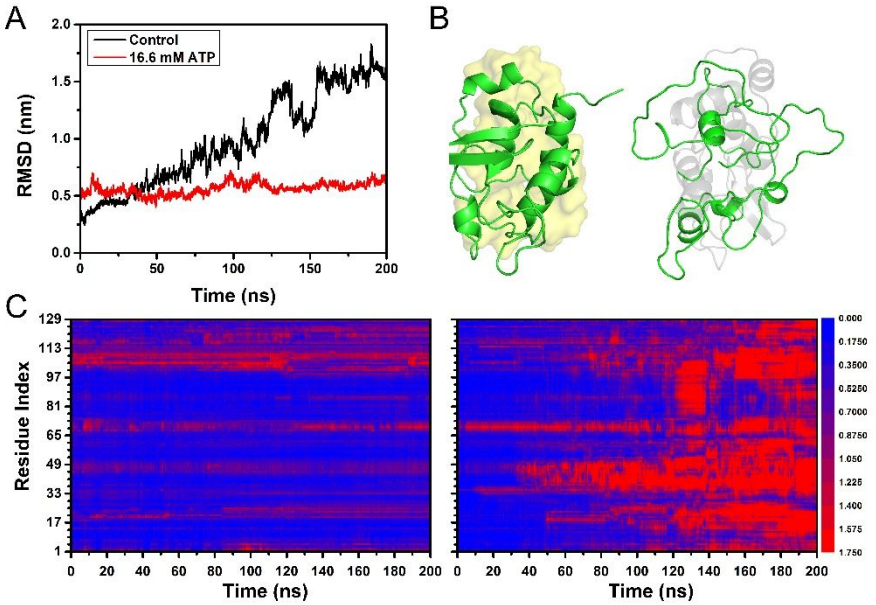

Figure S17. Structural characterization of free lysozyme and ATP-bound lysozyme in Mg^{2+}-free ATP solution (150 mM NaCl) at T = 430 K. (A) RMSD of free protein and ATP-bound protein with respect to the crystal structure. (B) Representative snapshot of the free protein (right panel, the native structure is shown in shaded grey) and ATP-bound protein (left panel, ATP-clusters are shown in shaded yellow). (C) RMSD of residues of the free protein (right panel) and ATP-bound protein (left panel). The color scale represents the range of RMSD.

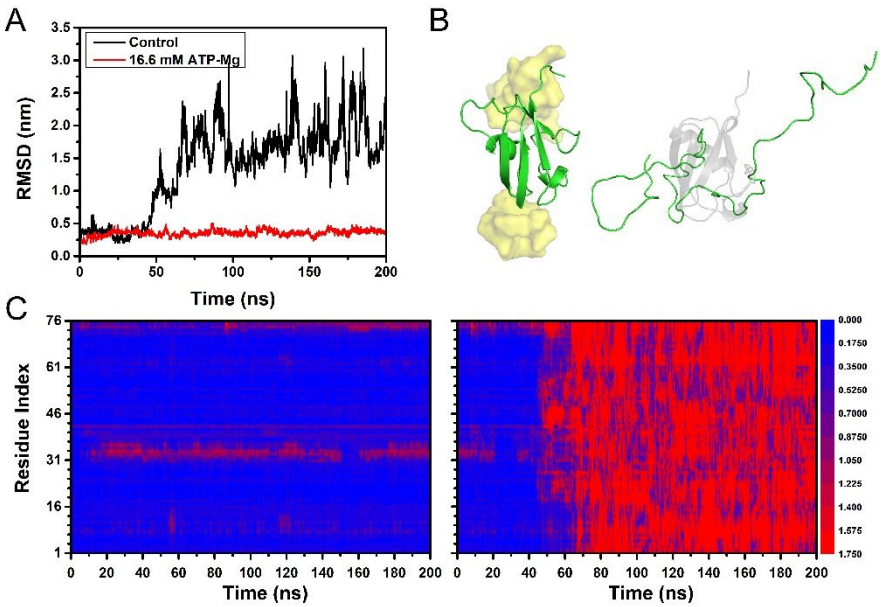

Figure S18. Structural characterization of free ubiquitin and ATP-bound ubiquitin at T = 490 K. (A) RMSD of free protein and ATP-bound protein with respect to the crystal structure. (B) Representative snapshot of the free protein (right panel, the native structure is shown in shaded grey) and ATP-bound protein (left panel, ATP-clusters are shown in shaded yellow). (C) RMSD of residues of the free protein (right panel) and ATP-bound protein (left panel). The color scale represents the range of

RMSD.

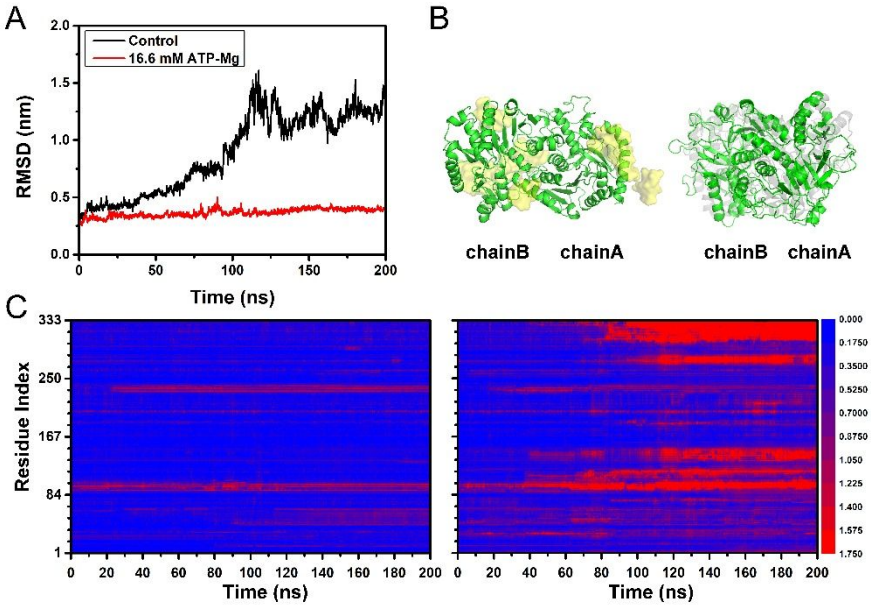

Figure S19. Structural characterization of free malate dehydrogenase and ATP-bound malate dehydrogenase at T = 450 K. (A) RMSD of chain A of the free protein and ATP-bound protein with respect to the crystal structure. (B) Representative snapshot of the free protein (right panel, the native structure is shown in shaded grey) and ATP-bound protein (left panel, ATP-clusters are shown in shaded yellow). (C) RMSD of residues of chain A of the free protein (right panel) and ATP-bound protein (left panel). The color scale represents the range of RMSD.

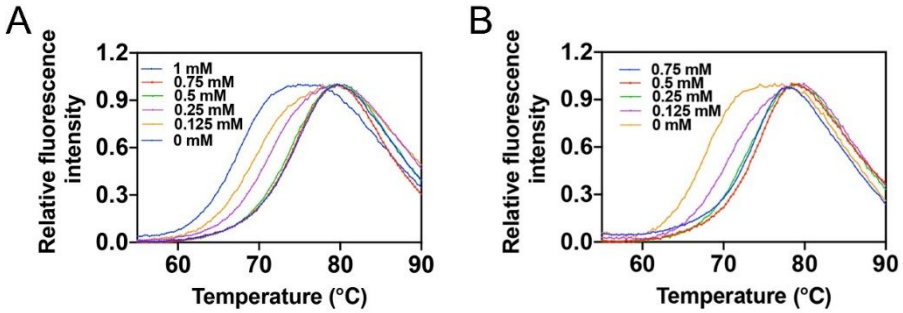

Figure S20. (A) Typical normalized melting curves for lysozyme at varied ATP-Mg concentrations. (B) Typical normalized melting curves for lysozyme at varied ATP concentrations in *Mg^{2+}-free ATP solution*.

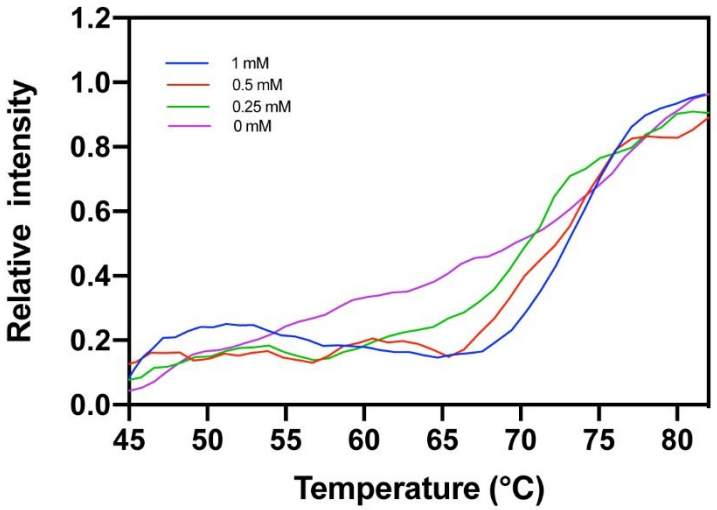

Figure S21. Circular dichroism spectra. The thermally induced ellipticity changes at 222 nm for lysozyme in the solutions with various ATP-Mg concentrations.

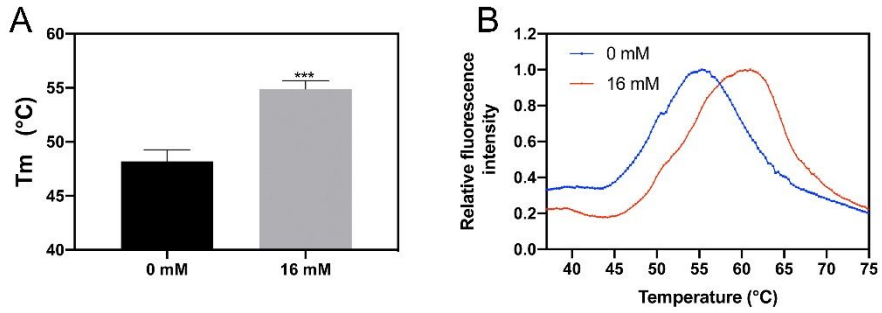

Figure S22. Thermal shift assay for malate dehydrogenase. (A) The relationship of the melting temperature with ATP-Mg concentration. (B) Typical normalized melting curves.

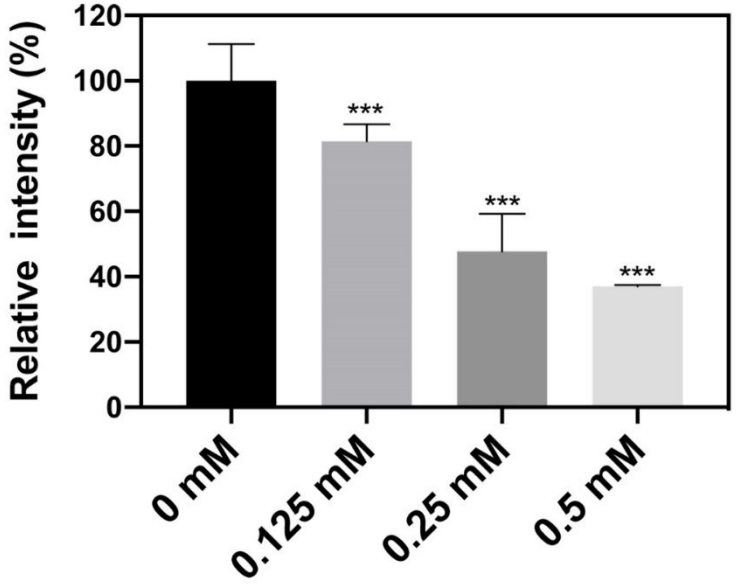

Figure S23. The summarized ANS fluorescence intensity for lysozyme in the solutions

with various ATP-Mg concentrations.